On Compact RAC Drawings

Henry Förster
Wilhelm-Schickard-Institut für Informatik, University of Tübingen, Germany
foersth@informatik.uni-tuebingen.de

Michael Kaufmann
Wilhelm-Schickard-Institut für Informatik, University of Tübingen, Germany
mk@informatik.uni-tuebingen.de

Abstract

We present new bounds for the required area of Right Angle Crossing (RAC) drawings for complete graphs, i.e. drawings where any two crossing edges are perpendicular to each other. First, we improve upon results by Didimo et al. [15] and Di Giacomo et al. [12] by showing how to compute a RAC drawing with three bends per edge in cubic area. We also show that quadratic area can be achieved when allowing eight bends per edge in general or with three bends per edge for p-partite graphs. As a counterpart, we prove that in general quadratic area is not sufficient for RAC drawings with three bends per edge.

2012 ACM Subject Classification Mathematics of computing → Graphs and surfaces; Theory of computation → Graph algorithms analysis; Mathematics of computing → Graph algorithms; Human-centered computing → Graph drawings

Keywords and phrases RAC drawings, visualization of dense graphs, compact drawings

Digital Object Identifier 10.4230/LIPIcs.ESA.2020.53

Acknowledgements We thank Patrizio Angelini for useful discussions and proofreading and the anonymous referees of an earlier version for helpful comments.

1 Introduction

Graphs that appear in real-world applications are in fact mostly nonplanar. Experiments on the human perception of graph drawings indicate that two important parameters affecting readability are angles formed by two edges at their crossing points (the larger the better) [20, 21] as well as the number of bends along an edge (the fewer the better) [24, 25]. The first theoretical drawing model that has taken these experimental results into account is the so-called *RAC* (or *right-angle-crossing*) drawing introduced in [15]. In some sense, the RAC model generalizes the popular orthogonal graph drawing model [17]. Formally, a RAC drawing is a node-link drawing of a graph, in which edges are drawn as polylines so that the angles formed at the crossing points of two edges are always equal to $\pi/2$. Since a RAC drawing is a geometric embedding, in most studies on RAC drawings the number of bends per edge has also been taken into account. In the following, we denote a RAC drawing with at most k bends per edge as a *RAC_k drawing*.

Many main research questions of graph drawing have been studied for RAC drawings. Regarding their density, already Didimo et al. [15] showed that graphs admitting straight-line RAC drawings have at most $4n-10$ edges, which is a tight bound. They also showed that the density for graphs admitting RAC_1 or RAC_2 drawings is subquadratic, whereas all graphs admit a RAC_3 drawing. Subsequently, Arikushi et al. [6] showed that graphs admitting a RAC_1 drawing can only have $6.5n-13$ edges, while graphs admitting RAC_2 drawings can have at most $74.2n$ edges; the former bound for RAC_1 drawings was recently improved by Angelini et al. [2] to $5.5n-11$. The recognition problem for graphs admitting straight-line RAC drawings is known to be NP-hard [5], even in the case where the resulting drawing must

Table 1 Overview of area bounds on RAC drawings of general graphs.

Known Results			**Our New Results**	
RAC_3:	$\mathcal{O}(n^4)$	[15]	RAC_3:	$\mathcal{O}(n^3)$
RAC_4:	$\mathcal{O}(n^3)$	[12]	RAC_3 (p-partite):	$\mathcal{O}(p^4n^2)$
$RAC_{\geq 3}$:	$\Omega(n^2)$	[15]	RAC_3:	$\omega(n^2)$
RAC_6:	$\mathcal{O}(n^{2.75})$	[26]	RAC_8:	$\mathcal{O}(n^2)$

be upward [3] or 1-planar [8]. Note that a k-planar graph is a graph which admits a drawing where every edge is crossed at most k times. While the recognition of graphs admitting RAC_3 drawings is trivial, the corresponding problem for graphs admitting RAC_1 or RAC_2 drawings is yet unsettled. Curiously, the maximally dense graphs admitting straight-line RAC drawings have been shown to be 1-planar [18]. In addition, subclasses of 1-planar graphs have been investigated: Brandenburg et al. [9] proved that all IC-planar graphs admit a straight-line RAC drawing, which has been shown to be not true for NIC-planar graphs [7]. IC-planar and NIC-planar graphs are graphs with a 1-planar drawing where the set of vertices involved in a crossing shares at most zero and one vertices with the set of vertices involved in a different crossing, respectively. Di Giacomo et al. [11] and Hong and Nagamochi [19] studied variants of RAC drawings with restricted vertex positioning in the straight-line setting. Angelini et al. [3] showed that all graphs of maximum degree three admit a RAC_1 drawing, whereas graphs of maximum degree six admit a RAC_2 drawing.

To evaluate the area of RAC drawings, vertices and bends are assumed to be located on an integer grid. The area of a drawing then is the product of the number of horizontal and vertical grid lines appearing in a bounding axis-aligned rectangle. It is known that even planar graphs may still require quadratic area in any straight-line RAC drawing [3]. Recently, Chaplick et al. [10] showed that NIC planar graphs admit RAC_1 drawings in polynomial area, whereas 1-planar graphs admit RAC_2 drawings in polynomial area. The drawing algorithm by Didimo et al. [15] achieves RAC_3 drawings in $\mathcal{O}(n^4)$ area. Subsequently, Di Giacomo et al. [12] improved the area to $\mathcal{O}(n^3)$ for RAC_4 drawings and Rahmati and Emami [26] recently achieved $\mathcal{O}(n^{2.75})$ area for RAC_6 drawings. For the closely related family of *LAC graphs* (short for *large-angle-crossing*), in which edges may cross at angles at least $\pi/2 - \varepsilon$ for some small $\varepsilon > 0$, Di Giacomo et al. [12] also showed that the complete graph on n vertices admits a drawing with one bend per edge in $\mathcal{O}(n^2(\cot \varepsilon/2)^2)$ area, which can be assumed to be $\mathcal{O}(n^2)$ area for fixed values of ε. Note however that for very small values of ε such as $\pi/180$, the multiplicative constant is very large and may therefore be infeasible in practise. For further results on LAC drawings see also [4, 16].

It is noteworthy that these drawing algorithms only place vertices and bends on an integer grid while crossings may occur on non-grid points. The positions of crossings are implicitly defined by the positions of endpoints of the intersecting segments. Since by the crossing lemma [1, 22] there are $\Omega(n^4)$ crossings in the complete graph K_n, it is impossible to achieve an area bound of $o(n^4)$ if also the crossings are required to be on the grid. In the variant where crossings are located on the grid, the algorithm by Didimo et al. [15] for RAC_3 drawings in $\mathcal{O}(n^4)$ area yields optimal solutions. We emphasize that it is not trivial to compute RAC drawings with $\mathcal{O}(n^2)$ area with additional bends as only $\mathcal{O}(1)$ bends per edge can fit in $\mathcal{O}(n^2)$ area. Finally, tradeoffs between area and planar thickness [14] as well as number of crossings per edge [13] also have been investigated.

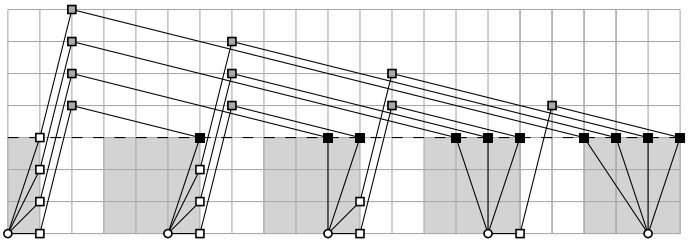

Figure 1 RAC_3 drawing of K_5 in 21×7 area.

We emphasize that we study *simple* graphs on n vertices, i.e., graphs without self-loops and parallel edges. The restriction to simple graphs is common in this line of research as each edge connecting the same vertices must be assigned distinct positions for its bends. In Section 2, we give new area upper bounds. We prove that every graph admits a RAC_3 drawing in $\mathcal{O}(n^3)$ area improving the known bound by a factor of n. Also, we show that even $\mathcal{O}(n^2)$ area can be achieved when eight bends per edge are allowed or when the input graph is p-partite. Then, in Section 3, we prove that quadratic area cannot be achieved in general for RAC_3 drawings. See also Table 1 for an overview of our new results compared to results from the literature. We conclude the paper with some open problems.

2 New Area Upper Bounds for RAC Drawings

▶ **Theorem 1.**

1. *Every n-vertex graph $G = (V, E)$ admits a RAC_3 drawing in $\mathcal{O}(n^3)$ area.*
2. *Every n-vertex graph $G = (V, E)$ admits a RAC_8 drawing in $\mathcal{O}(n^2)$ area.*
3. *Every p-partite n-vertex graph $G = (V, E)$ admits a RAC_3 drawing in $\mathcal{O}(p^4 n^2)$ area.*

Proof (of Result 1). Our algorithm is a refinement of the algorithm by Didimo et al. [15]. Note that it is easy to see that the drawings produced by the algorithm in [15] require $\Theta(n^4)$ area as two bends for each edge are located on a horizontal line.

For an example of a drawing of K_5 refer to Fig. 1. The vertices and the segments incident to vertices are drawn planar in a disjoint region of quadratic area for each vertex; see the gray regions in Fig. 1. In contrast to [15], each vertex (except for the outermost two) is incident to two types of bends (white and black squares in Fig. 1) which lead to vertices with larger and smaller indices, resp. The remaining two segments of edges use nearly horizontal or nearly vertical slopes.

We number the vertices arbitrarily from 0 to $n-1$. We place vertex v_i at position $(i \cdot n, 0)$; see white disks in Fig. 1. The three bends of edge (v_i, v_j) with $i < j$ are placed as follows: Bend $a_{i,j}$ connected to v_i is placed at $(i \cdot n + 1, j - i - 1)$; see white squares in Fig. 1. The middle bend $b_{i,j}$ is placed at $(i \cdot n + 2, n + j - i - 2)$; see gray squares in Fig. 1. Bend $c_{i,j}$ connected to v_j is placed at $(j \cdot n - j + i + 2, n - 2)$; see black squares in Fig. 1.

It remains to show that the resulting drawing is indeed RAC. Consider the start segments incident to vertex v_i, i.e., segments of types $(v_i, a_{i,j})$ for $(v_i, v_j) \in E$ and $(v_i, c_{j,i})$ for $(v_j, v_i) \in E$. Together with v_i they form a *fan* and do not intersect each other as the bend points of types $a_{i,j}$ and $c_{j,i}$ are distinct. Note that while $a_{0,n-1}$ is located at $(1, n-2)$, for other vertices v_i the bend $c_{i-1,i}$ is located at $(i \cdot n + 1, n - 2)$. These fans are drawn in disjoint *start regions* (gray shaded areas in Fig. 1); more precisely, the fan of v_i is located within a rectangle ranging from 0 to $n-2$ in y-direction and from $(i-1) \cdot n + 3$ to $i \cdot n + 1$ in x-direction. Since all segments $(b_{i,j}, c_{i,j})$ are located above the start regions and because

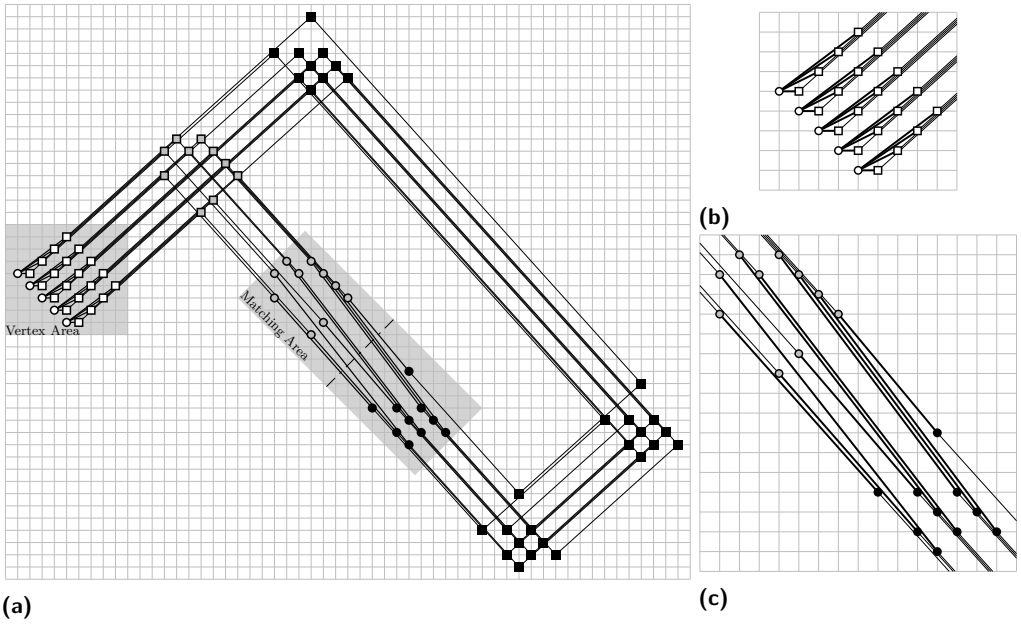

Figure 2 (a) RAC_8 drawing of K_5 in 55×47 area, (b)–(c) zoom into vertex and matching area.

segments $(a_{i,j}, b_{i,j})$ are located between x-coordinates $i \cdot n + 1$ and $i \cdot n + 2$ (i.e., they are located between two start regions), there are no crossings within start regions. As all crossings occur between segments of type $(a_{i,j}, b_{i,j})$ (which have slope $n - 1$) and $(b_{i,j}, c_{i,j})$ (which have slope $-1/(n-1)$), all proper crossings are at right angles.

It remains to prove that there are no overlaps. Recall that bend points in each start region are distinct, hence, we consider only the remaining segments. Segments of edges with a common endpoint cannot overlap. As the regions containing edges $(a_{i,j}, b_{i,j})$ and $(a_{k,l}, b_{k,l})$ for $i \neq k$ are disjoint, overlaps may only occur at segments $(b_{i,j}, c_{i,j})$ and $(b_{k,l}, c_{k,l})$ for some $i \neq k$. Since both segments have the same slope and their crossings with the horizontal at $y = n - 2$ (dashed in Fig. 1) are distinct (i.e., $c_{i,j}$ and $c_{k,l}$), they also do not overlap.

As the lowest x- and y-coordinates are both 0 whereas the largest x- and y-coordinates are $(n-1)n + 1$ and $2n - 3$, resp., the area bound follows.

Proof (of Result 2). We describe how to draw K_n for odd n in quadratic area. For even n, refer to the construction of K_{n+1}. For an example of a drawing of K_5 refer to Fig. 2. We number the vertices arbitrarily from 0 to $n - 1$. The general idea is as follows: vertices and start segments are located in the *vertex area* such that each start segment bend is connected to a segment whose slope is slightly less than 1; see Fig. 2b. Edges are treated as two half edges that are routed to the *matching area* independently with segments of slopes s and $-1/s$. One half edge is routed to the top left half of the matching area (gray bends in Fig. 2a) and the other half edge is routed to the bottom right half (black bends in Fig. 2a). In the matching area half edges are matched crossing-free realizing an edge for each pair of vertices; see Fig. 2c. We point out that in principle each half edge may be routed to either half of the matching area. When we define the matching of the bends in the matching area, we will show which half edges have to be routed to which half of the matching area.

We place vertex v_i at position $(i, -i)$; see white circles in Fig. 2b. Let e_i^j be the j-th half edge incident to vertex v_i for $0 \leq j < n - 2$. We place the bend of e_i^j that is closest to v_i at $(i + j + 1, j - i)$; see white squares in Fig. 2b. Bends incident to the same vertex v_i are

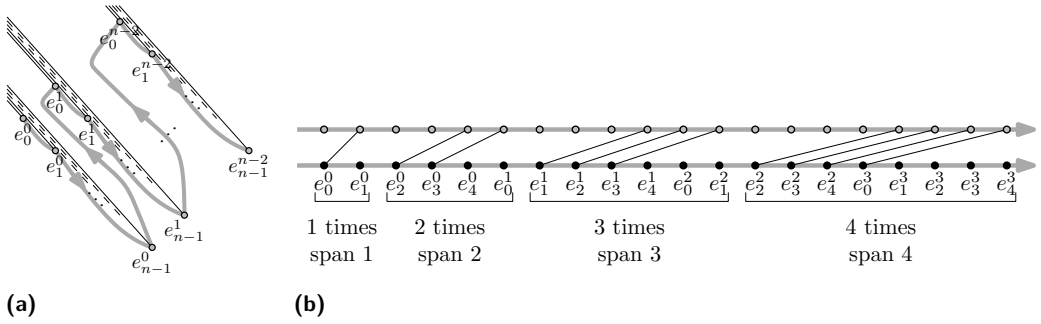

Figure 3 (a) Accessability of matching bends in the top left half of the matching area, and (b) matching assignment for $n = 5$ used for the drawing in Fig. 2.

located on a diagonal of slope 1 and all start segments of v_i are above this diagonal. Since v_i is located below the diagonal of vertex v_{i-1}, start segments do not intersect each other and all $n \cdot (n-1)$ start segment bends are within a rectangle of quadratic area tilted by $\pi/4$.

We choose $s = (2n-1)/2n$ achieving the following: If $n \cdot (n-1)$ bends are located in a rectangle R as defined by the start segment bends and a segment of slope s is added to each of these points, the next integer point used by any of those segments is located outside of R. This procedure "copies" the bends at $k \cdot 2n$ horizontal and $k \cdot (2n-1)$ vertical distance for $k \in \mathbb{Z}$. A similar property holds for segments of slope $-1/s$. Further, since s is slightly less than 1 and start segments are above the line of slope 1 through start segment bends, those additional segments of slope s do not intersect any start segment; see Fig. 2b. In the matching area all bends in the top left (bottom right, resp.) half are accessible from the bottom right (top left, resp.) without intersections; see Fig. 2c.

Next, we define the bend points of half edge e_i^j leading from vertex to matching area. Recall that the bend in the vertex area (white squares in Fig. 2a) is at $(i+j+1, j-i)$. If e_i^j is routed to the top left half of the matching area, we place one bend at $(2n+i+j+1, 2n+j-i-1)$ (gray squares in Fig. 2a) and enter the matching area with a bend at $(4n+i+j, j-i-1)$ (see gray circles in Fig. 2a). If e_i^j is routed to the bottom right half of the matching area, we instead create a sequence of three bends at $(4n+i+j+1, 4n+j-i-2)$, $(10n+i+j-2, -2n+j-i-2)$ and $(8n+i+j-2, -4n+j-i-1)$ (see black squares in Fig. 2a) and enter the matching area with a bend at $(6n+i+j-1, -2n+j-i-1)$ (see black circles in Fig. 2a). The leftmost x-coordinate is 0 (for vertex v_0), while the rightmost one is $12n-5$ (for a bend of e_{n-1}^{n-2}). Conversely, the topmost y-coordinate is $5n-4$ (for a bend of e_0^{n-2}) while the bottommost one is $-5n$ (for a bend of e_{n-1}^0). Hence, the drawing requires $(12n-5) \times (10n-3)$ area.

It remains to show that *matching segments* between matching bends are crossing-free. Consider the accessibility of matching bends from the other half of the matching area: Each matching bend in the top left half of the matching area is accessible from below the diagonal of slope -1 passing through it, since from above its incident segment of slope $-1/s$ is forming an obstacle. A similar statement is true for matching bends in the bottom right half of the matching area. We can use this observation to define an ordering of the matching bends based on their accessability. The first accessible matching bend is of half edge e_0^0; i.e., incident to v_0, the second is of e_1^0; i.e., incident to v_1. This pattern continues increasing in i until all e_i^0 are encountered; see Fig. 3a. Afterwards, all e_i^1 are encountered, in increasing order of i. This pattern repeats increasing in j, until all half edges e_i^j are encountered, in increasing order of i; see Fig. 3a.

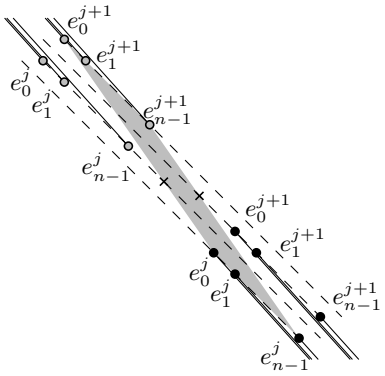

Figure 4 Area for drawing matching segments of half edges e_i^j and e_k^{j+1}.

We use the two linear orders of matching bends to define a planar matching between both halves of the matching area. Note that both linear orders are identical; see Fig. 3b. The matching that we define has two properties: First, the distance between matched bends in the linear order is bounded by $n-1$. Second, the matching ensures that every pair of vertices is connected exactly once. We now describe the specific matching: First, we connect the first matching bend of the bottom right half of the matching area with the second matching bend of the top left half of the matching area. Then, we connect the next two matching bends of the bottom right half of the matching area with the following two matching bends of the top left half of the matching area. We continue this pattern while always increasing the size of the groups of matched pairs by one which also increases the *span* of the matching segments, i.e., the distance between the connected matching bends in the linear order; see Fig. 3b. Then, there are exactly k matching segments of span k for all values $1 \leq k \leq n-1$. A matching segment of span k connects a vertex v_i whose bend is in the bottom right half of the matching area with vertex $v_{(i+k) \bmod n}$, i.e. with the neighbor whose index is k larger in the cyclic order of vertices. We prove that every pair of vertices is matched exactly once using that n is odd and that therefore the distance of vertices in the cyclic order is at most $(n-1)/2$. Due to cyclicity, segments with span $n-k > (n-1)/2$ correspond to a connection from vertex v_i in the top left half of the matching area to vertex $v_{(i-(n-k)) \bmod n} = v_{(i+k) \bmod n}$, i.e. again to the neighbor whose index is k larger in the cyclic order of vertices. Hence, for $k \leq (n-1)/2$, there are k segments of span k and $n-k$ segments of span $n-k$, which means that in total n vertices are matched to their neighbors whose indices are k larger. In order to see that all of them are distinct, we apply a recursive argument: Clearly, this is true for $k=1$. Assume that all matching segments of spans k and $n-k$ had different neighbors, then remove the matched bends that were matched with span k ($n-k$, resp.) from the left (right, resp.) end of the linear order. In total, we remove $2n$ vertices each from the ends of both linear orders, i.e., $2k$ from the left and $2(n-k)$ from the right, before finding the segments of spans $k+1$ and $n-(k+1)$. Thus, their endpoints differ.

Finally, we show that the matching segments are planar straight-line segments. First observe that since the span of segments is at most $n-1$, half edge e_i^j is matched with a half edge e_k^ℓ for $\ell \in \{j, j+1\}$. Further, notice that the diagonal on which the matching bends of the j-th half edges in the top left half of the matching area are located is halfway in between the corresponding diagonals for the matching bends of the j-th and $j+1$-th half edges in the bottom right half; see Fig. 4. We show that the intersection of the line through the bend of e_0^{j+1} in the top left half and the bend of e_0^j in the bottom right half of the matching area crosses the diagonal through the bends of e_0^j and e_{n-1}^j in the top left half of the matching

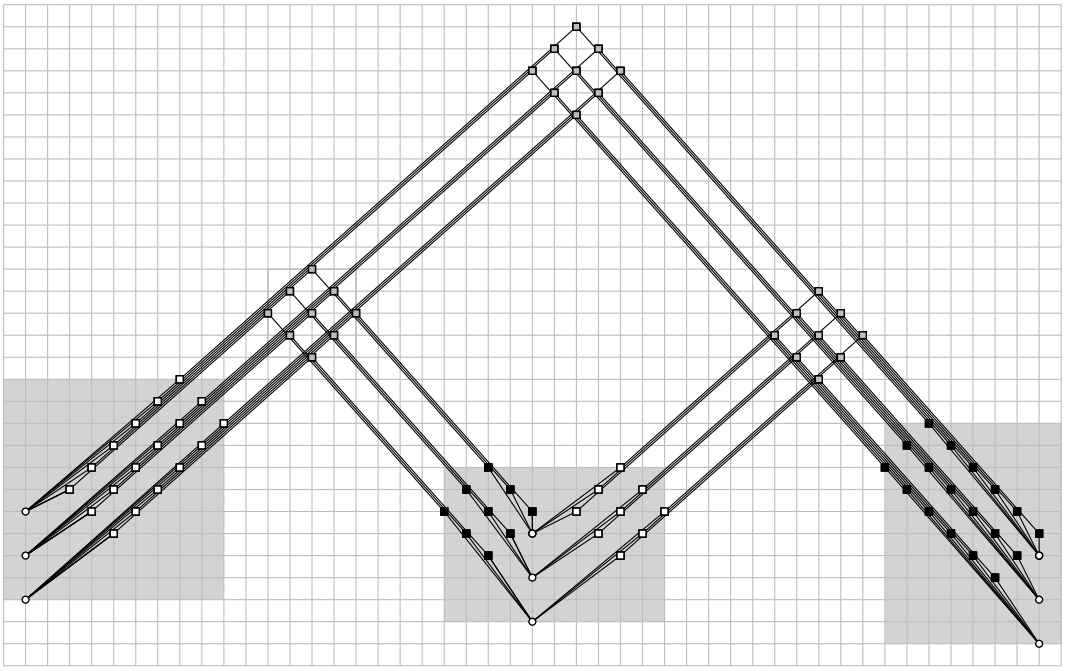

Figure 5 RAC_3 drawing of $K_{3,3,3}$ in 46×28 area.

area to the right of the bend of e^j_{n-1}; see crosses in Fig. 4. A symmetric property follows for bottom right half and consequently, segments between the j-th and $j+1$-th half edge are crossing-free. The first line goes through points $(4n+j+1, j)$ (bend of e^{j+1}_0 in the top left half of the matching area) and $(6n+j-1, -2n+j-1)$ (bend of e^j_0 in the bottom right half of the matching area) and hence has slope $-(2n+1)/(2n-2)$. The second line goes through point $(5n+j-1, -n+j)$ (bend of e^j_{n-1} in the top left half of the matching area) and has slope -1. We compute the two line equations based on the fact that we know a point on each line and the corresponding slopes:

$$y = -\frac{2n+1}{2n-2}x + \frac{8n^2+4nj+6n-j+1}{2n-2} \qquad \text{and} \qquad y = -x+4n+j+1$$

and the x-coordinate of the intersection point $x = 16/3n + j - 1/3$ that is to the right of the bend of e^j_{n-1} in the top left half of the matching area as claimed.

Proof (of Result 3). We describe how to draw $K_{(n_p)_p}$, the complete p-partite graph with n_p vertices per partition. Refer to Fig. 5 for an example drawing of $K_{3,3,3}$. If the partitions have different sizes, we augment the graph to $K_{(n_p)_p}$ where n_p is the number of vertices in the largest partition. Note that $n_p < n$ and $pn_p \geq n$. We number the partitions arbitrarily from 0 to $p-1$ and the vertices in each partition from 0 to $n_p - 1$. Let v^j_i denote the i-th vertex of the j-th partition.

We position vertex v^j_i at $(2pn_pj + 2n_pj - j, 2i - j)$; see white circles in Fig. 5. Edge (v^j_i, v^ℓ_k) with $j < \ell$ is drawn with the following three bends:

- The bend incident to vertex v^j_i is located at $(2pn_pj + n_p\ell + n_pj + k - i - j + 1, n_p\ell - n_pj + i + k - j)$; see white squares in Fig. 5.
- The middle bend is located at $(pn_p\ell + pn_pj + n_p\ell + n_pj + k - i - j + 1, pn_p\ell - pn_pj + n_p\ell - n_pj + i + k - \ell)$; see gray squares in Fig. 5.
- The bend incident to vertex v^ℓ_k is located at $(2pn_p\ell + n_p\ell + n_pj + k - i - \ell + 1, n_p\ell - n_pj + i + k - \ell)$; see black squares in Fig. 5.

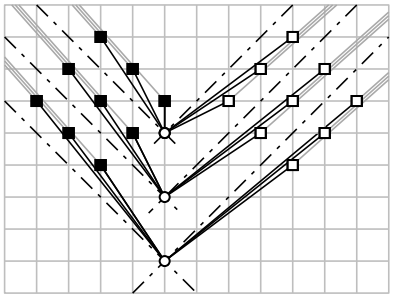

Figure 6 Detail of the vertex stars of the middle partition in Fig. 5.

The lowest x-coordinate assigned is 0 (for vertices in partition 0), while the highest x-coordinate assigned is $2p^2n_p - 2n_p - p + 1$ (for vertices in partition $p-1$). Conversely, the lowest y-coordinate is $-p+1$ (for vertex v_0^{p-1}) whereas the largest y-coordinate is $p^2n_p + n_p - p - 1$ (for the middle bend of edge $(v^0_{n_p-1}, v^{p-1}_{n_p-1})$). Since $pn_p \leq pn$, it follows, that the total area is $\mathcal{O}(p^4n^2)$.

It remains to discuss that the resulting drawing is RAC. First we have a look at the segments incident to the middle bend (i.e., the segments which are not start segments). All of these segments have slopes $(n-1)/n$ (between white and gray squares in Fig. 5) or $-n/(n-1)$ (between black and gray squares in Fig. 5). Hence, each pair of these segments is either parallel or perpendicular.

Next, we show that start segments of different partitions do not intersect; see gray shaded areas in Fig. 5. To see this, we consider the rightmost bend incident to a vertex of partition j and the leftmost incident to a vertex of partition ℓ such that $j < \ell$. The rightmost bend of partition j belongs to edge $(v_0^j, v^{p-1}_{n_p-1})$ and has x-coordinate $2pn_pj + pn_p + n_pj - j$ whereas the leftmost bend of partition ℓ belongs to edge $(v^0_{n_p-1}, v_0^\ell)$ and has x-coordinate $2pn_p\ell + n_p\ell - n_p - \ell + 2$, i.e., at least $2pn_pj + 2pn_p + n_pj - j + 1$ since $\ell \geq j+1$. Hence, the leftmost bend of partition ℓ is at least $pn_p + 1 \geq n+1$ units right of the rightmost bend of partition j. Hence, start segments from different partitions cannot intersect.

In addition, we establish that middle bends are located outside of vertex fans. To see this, consider the topmost bend of a vertex fan of partition j. This is either $y_r = pn_p + n_p - n_pj - j - 2$ (bend of edge $(v^j_{n_p-1}, v^{p-1}_{n_p-1})$) or $y_\ell = n_pj + 2n_p - j - 2$ (bend of edge $(v^0_{n_p-1}, v^j_{n_p-1})$). Since middle bends appear in groups of n_p^2 bends, we only consider the lowest of these bends which is always incident to two vertices v_0^a and v_0^b for some partitions a and b such that $b > a$. The y-coordinate of this bend is equal to $y_m = pn_p(b-a) + n_p(b-a) - b$. Clearly, $y_m \leq y_r$ is only possible if $(b-a) = 1$ and $b \geq j+2$ in which case the middle bends are between two partitions whose start segments are to the right of the start segments of partition j (and hence the middle bends are to the right as well). Also since $(b-a) \geq 1$, it holds that $y_m \geq pn_p + n_p - b$ and, since $b \leq p-1$, also $y_m \geq pn_p + n_p - p + 1$. However, even for $j = p-1$ it holds that $y_\ell = pn_p + n_p - p - 1$ and hence $y_\ell < y_m$.

Next, we show planarity for the start segments. We first observe that each vertex v_i^j is incident to two sets of bends, namely,

- those that belong to an edge (v_k^ℓ, v_i^j) for some $\ell < j$. These are located on a diagonal with slope -1 left of the vertex; see black squares in Fig. 5. We will refer to these as the *left bends* of the vertex fan.
- those that belong to an edge (v_i^j, v_k^ℓ) for some $\ell > j$. These are located on a diagonal with slope 1 right of the vertex; see white squares in Fig. 5. We will refer to these as the *right bends* of the vertex fan.

We will show that v_i^j is located on the intersection of the diagonal with slope -1 located one unit below the diagonal through its left bends and the diagonal with slope 1 located one unit above the diagonal through its right bends; see dashed diagonals in Fig. 6. Hence, the start segments do not intersect segments between its start segment bends and the corresponding middle bends. Also, since the latter "middle" segments have slope $(n-1)/n$ or $-n/(n-1)$ the start segments of vertex v_i^j do not intersect middle segments of vertices v_{i-1}^j and v_{i+1}^j (as their middle segments only intersect the diagonal defining the position of v_i^j after moving n or $n-1$ units to the left/right).

The diagonal located one unit below the left vertex fan bends passes through the point $p_\ell = (2pn_pj + n_pj + i - j + 1, n_pj + i - j - 1)$ (one unit below the bend of edge (v_0^0, v_i^j). It is easy to verify that $(2pn_pj + 2n_pj - j, 2i - j) = (1, -1) \cdot (n_pj - i - 1) + p_\ell$. Similarly, the diagonal located one unit above the right vertex fan bends passes through the point $p_r = (2pn_pj + 2n_pj + n_p - i - j + 1, n_p + i - j + 1)$ (one unit above the bend of edge (v_i^j, v_0^{j+1}). It holds that $(2pn_pj + 2n_pj - j, 2i - j) = (-1, -1) \cdot (n_p - i + 1) + p_r$ as required.

Next, we show that the start segments of partition j do not intersect the middle segments incident to a start segment bend of partition $\ell \neq j$. To do so, we show that the middle segments of partition ℓ are located above all start segments. Recall that the topmost y-coordinate of a right bend in j occurs on edge $(v_{n_p-1}^j, v_{n_p-1}^p)$ and is equal to $pn_p - n_pj + 2n_p - j - 2$, and that the topmost y-coordinate of a left bend in j occurs on edge $(v_{n_p-1}^0, v_{n_p-1}^j)$ and is equal to $n_pj + 2n_p - j - 2$. Thus, the topmost y-coordinate of any start segment bend is at most $pn_p + 2n_p - j - 2$. We consider two cases.

First, consider the case $\ell > j$. Further assume that $\ell = j + 1$ since the middle segments of partition $\ell' > \ell$ are located above those of partition ℓ. As established earlier, the horizontal distance between the start regions of partitions j and ℓ is at least $pn_p + 1$. Observe that at the leftmost x-coordinate of the start region of partition ℓ, we encounter the left bend of $(v_{n_p-1}^0), v_0^\ell)$ with y-coordinate $n_p\ell + n_p - \ell - 1 = n_pj + 2n_p - j - 2$. On the other hand, if we continue k units in x-direction, we have distance $pn_p + 1$ towards partition j and encounter a left bend with y-coordinate $n_pj + 2n_p - j - 2 - k$. Because the slope of middle segments incident to left bends is $-pn_p/(pn_p - 1)$, any such middle segment has y-coordinate at least $(pn_p+1+k)\cdot\frac{pn_p}{pn_p-1} + n_pj + 2n_p - j - 2 - k > pn_p + k + n_pj + 2n_p - j - 2 - k = pn_p + n_pj + 2n_p - j - 2$ which is larger than $pn_p + 2n_p - j - 2$. Hence, such a middle segment is above each start segment of region j.

Second, assume that $\ell < j$. Here, we can assume that $\ell = j - 1$ by a similar argument as before. Again, the horizontal distance between the start segment bends of partitions j and ℓ is at least $pn_p + 1$. At the rightmost x-coordinate that belongs to the start region of partition ℓ is the right bend of edge $(v_0^\ell, v_{n_p-1}^{p-1})$ with y-coordinate $pn_p - n_p\ell + n_p - \ell - 2 = pn_p - n_pj + 2n_p - j - 1$. If we continue k units in negative x-direction, we have a minimum distance of $pn_p + 1 + k$ towards partition j and encounter a left bend with y-coordinate $pn_p - n_pj + 2n_p - j - 1 - k$. Recall that the slope of middle segments incident to such bends is $(pn_p - 1)/pn_p$. Note that such middle segment has y-coordinate at least $(pn_p+1+k)\cdot\frac{pn_p-1}{pn_p} + pn_p - n_pj + 2n_p - j - 1 - k = 2pn_p - n_pj + 2n_p - j - 2 + -k/pn_p$ when above a start segment of region j. Since $k < jn_p$, we have that $2pn_p - n_pj + 2n_p - j - 2 + -k/pn_p > 2pn_p - n_pj + 2n_p - j - 2 + -j/p$. In addition, $j \leq (p-1)$ and we conclude that $2pn_p - n_pj + 2n_p - j - 2 + -j/p > pn_p + 3n_p - j - 2 - (p-1)(p)$ which is larger than $pn_p + 2n_p - j - 2$.

We conclude that middle segments of other partitions do not enter the start regions of other partitions. Finally, we only have to show that no two bends overlap and that no bend is located on an independent segment. First consider the start segment bends. Since middle bends are not inside vertex start regions, the only segments to consider here are the

middle segments incident to the same partition. These clearly do not overlap any of the start segment bends since the next grid points are located at least $n - 1 = pn_p - 1$ to the left/right while there are only at most $(p-1)n_p = pn_p - n_p$ bends each using consecutive x-coordinates.

Since the middle segments only shift the gridlike structure of start segment bends of the same partition, it follows, that no two bends of the same partition can overlap and that no bend is located on an independent segment from the same partition. Middle segments of two different partitions cannot overlap as well, as that would imply that one of the middle edges would pass through a start segment bend of the other partition. This is not possible since start segments of different partitions are at least $n + 1$ units horizontally apart from each other while their (consecutively pairwise) vertical distance is one. ◀

Since k-planar graphs are $\Theta(\sqrt{k})$-vertex colorable [23], we also obtain:

▶ **Corollary 2.** *Every n-vertex k-planar graph admits a (not necessarily k-planar) RAC$_3$ drawing in $\mathcal{O}(k^2n^2)$ area.*

3 An Area Lower Bound for RAC$_3$ Drawings

We show that $\mathcal{O}(n^2)$ area cannot be achieved for RAC$_3$ drawings in general. We give an outline of our proof by contradiction: First, we show there are $\Omega(n^2)$ edges that have $\Omega(n^4)$ crossings on two sets S_i and T_i of parallel segments of maximum cardinality, where segments in S_i are perpendicular to segments in T_i and may intersect. Moreover, there must exist $\Omega(n^2)$ edges with both a segment in S_i and in T_i. Then, we derive properties on the length of the segments in S_i and T_i depending on their slope. This allows us to subdivide the drawing area into a constant number of disjoint regions $\mathcal{R}$, which can contain only one endpoint of a segment from S_i or from T_i of the same edge. We then restrict the possible positions of vertices incident to such endpoints located in a region $R \in \mathcal{R}$. As a result, in Lemma 13, we obtain that the edges with both a segment from S_i and a segment from T_i induce a subgraph which is p-partite for some $p > 1$ except for a linear number of so-called complete edges. Based on this observation, in the proof of Theorem 14, we identify a complete subgraph which has too few edges with both a segment from S_i and from T_i leading to a contradiction.

▶ **Lemma 3.** *Let Γ be a RAC drawing of K_n with $\mathcal{O}(1)$ bends per edge. Then there exist two sets of parallel edge segments S_i and T_i with cardinalities $|S_i| = \Omega(n^2)$ and $|T_i| = \Omega(n^2)$ in Γ such that the segments of S_i are perpendicular to the segments of T_i.*

Proof. We use the following two properties: First, by the crossing lemma, there are $\Omega(n^4)$ crossings in any drawing of K_n. Second, all crossings appear between perpendicular edge segments. We partition the set of segments of the drawing based on their slopes. More precisely, for some $k \in \mathbb{N}$, there are $2(k+1)$ sets of edge segments $S_0, \ldots, S_k$ and $T_0, \ldots, T_k$ such that S_i and T_i are perpendicular to each other. W.l.o.g. also assume that $|S_i| \geq |T_i|$ and that $|T_i| \geq |T_{i+1}|$. Since each edge has $\mathcal{O}(1)$ bends, there are at most cn^2 segments assigned to either set S_i for a constant c. Then, $|S_0| + \sum_{i=1}^{k} |S_i| = cn^2$ or in other words $|S_0| = cn^2 - \sum_{i=1}^{k} |S_i|$. Hence, we obtain the following relation for the number of crossings:

$$\Omega(n^4) \leq cr(\Gamma) \leq |S_0||T_0| + \sum_{i=1}^{k} |S_i||T_i| = \left(cn^2 - \sum_{i=1}^{k} |S_i|\right)|T_0| + \sum_{i=1}^{k} |S_i||T_i|$$

$$= cn^2|T_0| - \sum_{i=1}^{k} (|T_0| - |T_i|)|S_i| \leq cn^2|T_0|$$

which implies that $|S_0| = \Omega(n^2)$ and $|T_0| = \Omega(n^2)$. ◀

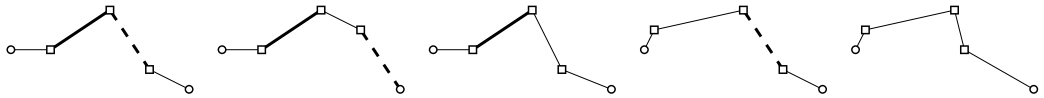

Figure 7 (a)–(b) Two edges belonging to E_i^{ST}, (c) an edge belonging to E_i^S, (d) an edge belonging to E_i^T, and, (e) an edge belonging to none of E_i^S, E_i^T and E_i^{ST}. Segments belonging to S_i are drawn bold and solid, segments belonging to T_i bold and dashed.

We show another property of edge sets contributing $\Omega(n^4)$ crossings. To this end, we consider all maximal sets of parallel edge segments that are involved in $\Omega(n^4)$ crossings and we partition these sets into two families $\mathcal{S} = \{S_1, \ldots, S_k\}$ and $\mathcal{T} = \{T_1, \ldots, T_k\}$ such that the segments in S_i and T_i are perpendicular while the segments in S_i and $S_j \cup T_j$ for $j \neq i$ are not. Observe that in contrast to the proof of Lemma 3, we now only consider segment sets S_i and T_i involved in $\Omega(n^4)$ crossings. Note that in a drawing with $\mathcal{O}(1)$ bends per edge, k is constant. In the following, we will discuss properties of pairs of sets $S_i \in \mathcal{S}$ and $T_i \in \mathcal{T}$. Let E_i^S (E_i^T, resp.) denote the set of edges with segments from S_i (T_i, resp.) but not from T_i (S_i, resp.), and E_i^{ST} the set of edges with segments from both S_i and T_i; see Fig. 7 for an illustration. In addition, let $E_{i,j}^{SX}$ denote the set of edges with segments from both S_i and from X_j where $X \in S, T$ and let $E_{i,j}^{TX}$ from both T_i and from X_j where $X \in S, T$. Note that $E_{i,i}^{ST} = E_i^{ST}$. The next lemmas show that there are S_i and T_i with $|E_i^{ST}| = \Omega(n^2)$.

▶ **Lemma 4.** *Let Γ be a RAC drawing of K_n with $\mathcal{O}(1)$ bends per edge. Then, there exists either sets $S_i \in \mathcal{S}$, $X_j \in \mathcal{S} \cup \mathcal{T}$ such that $|E_{i,j}^{SX}| = \Omega(n^2)$, or sets $T_i \in \mathcal{T}$, $X_j \in \mathcal{S} \cup \mathcal{T}$ such that $|E_{i,j}^{TX}| = \Omega(n^2)$.*

Proof. First, if $|E_{i,j}^{SX}| = \Omega(n^2)$ for some $S_i \in \mathcal{S}$ and $X_j \in \mathcal{S} \cup \mathcal{T}$ or if $|E_{i,j}^{TX}| = \Omega(n^2)$ for some $T_i \in \mathcal{T}$ and $X_j \in \mathcal{S} \cup \mathcal{T}$ with $i \neq j$; the lemma holds. Otherwise $|E_{i,j}^{SX}| = o(n^2)$ for all $S_i \in \mathcal{S}$ and $X_j \in \mathcal{S} \cup \mathcal{T}$ and $|E_{i,j}^{TX}| = o(n^2)$ for all $T_i \in \mathcal{T}$ and $X_j \in \mathcal{S} \cup \mathcal{T}$ with $i \neq j$. For a contradiction, also assume that $|E_i^{ST}| = o(n^2)$ for all $1 \leq i \leq k$. Hence, E_i^{ST} participates in $o(n^4)$ crossings. Also, assume w.l.o.g. that $|\bigcup_{i=1}^k E_i^S| \geq |\bigcup_{i=1}^k E_i^T|$. Consider the graph $G' = K_n \setminus \bigcup_{i=1}^k E_i^T$. Since G' contains $\bigcup_{i=1}^k E_i^S$, G' still has $\Omega(n^2)$ edges by Lemma 3. In Γ, there exists a valid subdrawing Γ' of G'. In Γ', by the crossing lemma, there still must be $\Omega(n^4)$ crossings between E_i^S and E_i^{ST} over all i. However, there are $o(n^4)$ crossings in Γ' from E_i^{ST} for $1 \leq i \leq k$; a contradiction for constant k. ◀

▶ **Lemma 5.** *Let Γ be a RAC$_3$ drawing of K_n. Then, $|E_{i,j}^{SX}| = o(n^2)$ for each pair of sets $S_i \in \mathcal{S}$, $X_j \in \mathcal{S} \cup \mathcal{T}$ with $i \neq j$ and $|E_{i,j}^{TX}| = o(n^2)$ for each pair of sets $T_i \in \mathcal{T}$, $X_j \in \mathcal{S} \cup \mathcal{T}$ with $i \neq j$.*

Proof. Assume w.l.o.g. that $|E_{i,j}^{ST}| = \Omega(n^2)$. Since only two start segments per vertex can belong to S_i and T_j, respectively, there are $\Omega(n^2)$ edges in $E_{i,j}^{ST}$, where the segments from S_i and T_j are not start segments. Let $\tilde{E}_{i,j}^{ST}$ denote this set of edges. Consider the start segments of $\tilde{E}_{i,j}^{ST}$ and let $\mathcal{P}_{start} = \{P_1, \ldots, P_r\}$ be a partitioning of the start segments into maximal sets of parallel segments. Since each vertex can be incident to only two start segments of the same slope, it follows that $|P_\ell| = \mathcal{O}(n)$ for all $1 \leq \ell \leq r$. Hence, there are only $\mathcal{O}(n^2)$ intersections between a perpendicular pair of start segments in $\tilde{E}_{i,j}^{ST}$. Similarly, if P_ℓ is perpendicular to S_i or T_j, it takes part in only $\mathcal{O}(n^3)$ intersections.

Consider the subgraph G' induced by $\tilde{E}_{i,j}^{ST}$. Note that G' has $\Omega(n^2)$ edges and hence by the crossing lemma it must have $\Omega(n^4)$ crossings. However, as established earlier, the subdrawing in Γ of G' only has $\mathcal{O}(n^3)$ intersections; a contradiction. ◀

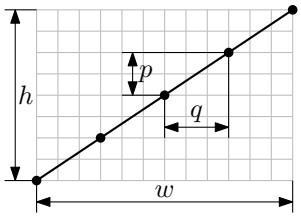

Figure 8 A fine-horizontal grid line (bold) with slope p/q, and its shared points with the coarse grid (gray lines).

The following lemma summarizes Lemmas 4 and 5.

▶ **Lemma 6.** *Let Γ be a RAC$_3$ drawing of K_n. Then, there exists a pair of sets $S_i \in \mathcal{S}$, $T_i \in \mathcal{T}$ such that $|E_i^{ST}| = \Omega(n^2)$, for some $1 \leq i \leq k$; i.e., $|E_i^{ST}| \geq c_{ST} n^2$ for an appropriate constant c_{ST} and sufficiently large n.*

Next, we investigate one pair of perpendicular segment sets $S_i \in \mathcal{S}$ and $T_i \in \mathcal{T}$. In the following analysis and all illustrations, we assume w.l.o.g. that the slope of segments in S_i is positive. First, we show that segments in S_i and T_i follow the grid lines of a finer grid that is tilted w.r.t. the coarse integer grid containing vertices and bends; see Fig. 8. We use this to show that segments in S_i and T_i are long w.r.t. the smaller side of the bounding rectangle.

▶ **Lemma 7.** *Let Γ be a RAC drawing of K_n with height h and width w and with $\mathcal{O}(1)$ bends per edge. Also, let $s = p/q$ be the slope of segments in $S_i \in \mathcal{S}$ for coprime integers p and q. Then,*

1. $\max\{p, q\} \in \Omega\left(\sqrt{n^4/(w \cdot h)}\right)$ *or* $pq \in \Omega\left(n^4/\max\{w^2, h^2\}\right)$*; and*
2. $p, q \in \mathcal{O}(\min\{w, h\})$.

Proof. Since the endpoints of each segment are grid points, the slope s_i of segments in S_i and the slope $-1/s_i$ of segments in T_i are rational numbers. Hence, the intersections between S_i and T_i are located at points with rational coordinates. By scaling the grid appropriately (i.e., by the factor of $p^2 + q^2$), we achieve integer coordinates for the intersections. In other words, all intersections are located on a *fine grid* while vertices and bends are on the integer grid which we call the *coarse grid*.

More precisely, the fine grid is defined by the *fine-horizontal* grid lines of slope s_i and by the *fine-vertical* grid lines of slope $-1/s_i$ each passing through at least two of the $h \cdot w$ vertices of the coarse grid. Note that by definition all vertices of the coarse grid are also vertices of the fine grid. Depending on the values of p and q, we observe that fine grid lines may pass through more than two points of the coarse grid; see Fig. 8. This limits how many fine grid lines exist. To see this, consider two consecutive fine-horizontal grid lines ℓ_1 and ℓ_2. Both lines ℓ_i (for $i \in \{1, 2\}$) can be expressed by a line formula of form $y = p/q \cdot x + b_i$. Since each line passes through integer points it holds that $b_i = 1/q \cdot c_i$ for some $c_i \in \mathbb{Z}$. More precisely, since ℓ_1 and ℓ_2 are consecutive, $|c_2 - c_1| = 1$ and the vertical distance between two consecutive fine-horizontal grid lines is $1/q$. In addition, we can compute the horizontal distance at the same y-coordinate by setting $p/q \cdot x_1 + b_1 = p/q \cdot x_2 + b_2$. Solving this equation yields $|x_2 - x_1| = q/p \cdot |b_2 - b_1| = 1/p \cdot |c_2 - c_1| = 1/p$ implying that the horizontal distance between two consecutive fine-horizontal grid lines is $1/p$. Analogously, the horizontal (vertical, resp.) distance between two fine-vertical grid lines is $1/q$ ($1/p$, resp.). Thus, there are at most $\Theta(\max\{wp, hq\})$ fine-horizonal and $\Theta(\max\{wq, hp\})$ fine-vertical grid lines.

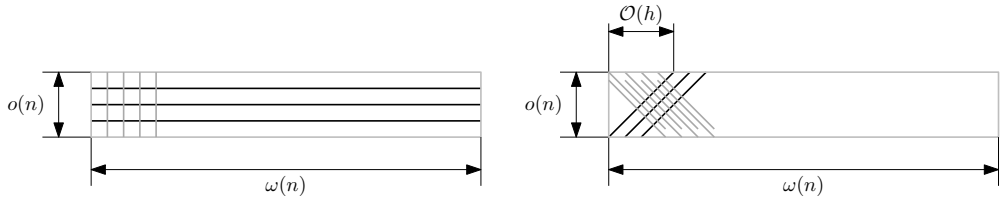

Figure 9 Proof of Lemma 8. If the area is $\omega(n) \times o(n)$, (a) there are $o(n)$ fine-horizontal grid lines (black), or, (b) fine-horizontal grid lines intersect $\mathcal{O}(h^2)$ fine-vertical grid lines (gray) each.

These two sets of grid lines intersect in $\Theta(\max\{w^2pq, whp^2, whq^2, h^2pq\})$ grid points, which must be $\Omega(n^4)$, the required number of crossings. Thus, $\max\{p,q\} \in \Omega\left(\sqrt{n^4/(w \cdot h)}\right)$ or $pq \in \Omega\left(n^4/\max\{w^2, h^2\}\right)$ which yields Property 1 of the lemma. Since the endpoints of all segments are located on the coarse grid, both $h, w \geq \max\{p,q\}$, which implies Property 2. ◀

The following lemma refines Lemma 7 for $\mathcal{O}(n^2)$ area and shows that both width and height are $\mathcal{O}(n)$ while segments in S_i and T_i have $\Omega(n)$ length.

▶ **Lemma 8.** *Let Γ be a RAC drawing of K_n with height h and width w and with $\mathcal{O}(1)$ bends per edge in $\mathcal{O}(n^2)$ area. Also, let p/q be the slope of segments in S_i such that p and q are coprime. Then,*

1. $h, w \in \Theta(n)$, *and,*
2. $\max\{p,q\} \in \Theta(n)$.

Proof. Assume for a contradiction that $h = o(n)$, i.e., $w = \omega(n)$. By Lemma 7,

1. $\max\{p,q\} \in \Omega\left(\sqrt{n^4/(w \cdot h)}\right) = \Omega(n)$ or $pq \in \Omega(n^4/\max\{w^2, h^2\}) = \Omega(h^2)$; and
2. $p, q \in \mathcal{O}(\min\{w, h\}) = \mathcal{O}(h)$

hold. By Property 2, it can only be $pq \in \Omega(h^2)$ but not $\max\{p,q\} \in \Omega(n)$. Consider the fine grid as defined in the proof of Lemma 7. First, if the fine-horizontal grid lines are in fact horizontal (i.e., $p = 0$), there can only be $\mathcal{O}(h)$ fine-horizontal grid lines since the height of the drawing is $\mathcal{O}(h)$; see Fig. 9a. Otherwise, the slope of the fine-horizontal grid lines is not horizontal. Recall that $p, q \in \mathcal{O}(h)$ since the height of the drawing is $\mathcal{O}(h)$. Since $pq = \Omega(h^2)$, $p, q \in \Theta(h)$. Hence, fine-horizontal grid lines have only length $\mathcal{O}(h)$ inside the bounding box and can only be crossed by $\mathcal{O}(h^2)$ fine-vertical grid-lines each; see Fig. 9b. Since $h = o(n)$, it is impossible to achieve $\Omega(n^4)$ crossings as in total there are only $\Theta(n^2)$ fine-horizontal grid lines. Thus, the assumption $h = o(n)$ leads to a contradiction. It follows that $h = \Theta(w)$, and hence, $w \in \Theta(n)$ and $\max\{p,q\} \in \Theta(n)$. ◀

So far, we considered properties of RAC drawings with $\mathcal{O}(1)$ bends per edge. The remaining results in this section hold specifically for RAC_3 drawings. Next, we explore connections realizable with edges in E_i^{ST} for a pair of perpendicular sets of segments $S_i \in \mathcal{S}$ and $T_i \in \mathcal{T}$. Based on slope p_i/q_i of segments in S_i for coprime integers p_i and q_i, consider a checkerboard partitioning of the drawing area into a set of square-shaped disjoint regions $\mathcal{R}_i$ of side length $\max\{p_i, q_i\}/2$ each. By Lemma 8, $\max\{p_i, q_i\} \in \Theta(n)$ and $h, w \in \Theta(n)$; and hence $|\mathcal{R}_i| = \mathcal{O}(1)$. By the choice of the slope, the length of segments in S_i have to be multiples of $\sqrt{p_i^2 + q_i^2}$. In particular, each segment in S_i has length larger than $\max\{p_i, q_i\}$. Due to the length of segments in S_i and the size of regions, we observe the following:

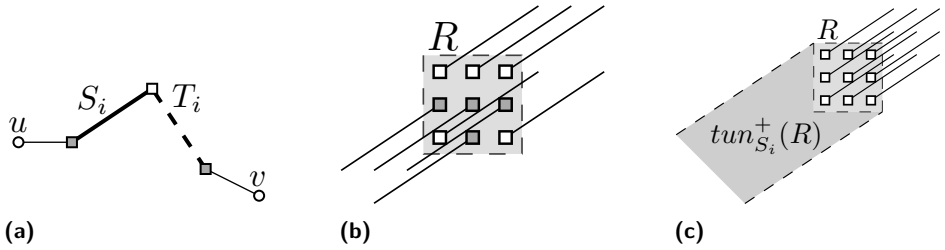

Figure 10 (a) An edge (u, v) whose middle segments (bold) belong to perpendicular set of segments $S_i \in \mathcal{S}$ and $T_i \in \mathcal{T}$. The gray bend incident to u (v, resp.) is an $S_i(T_i$, resp.)-endpoint. (b) A region R with set of bends $ep^+_{S_i}(R)$ (white squares) and set of bends $ep^-_{S_i}(R)$ (gray squares). (c) A region R with set of bends $ep^+_{S_i}(R)$ (white squares), their corresponding S_i-segments, and $tun^+_{S_i}(R)$.

▶ **Observation 9.** *At most one endpoint of a segment in S_i or T_i is in region $R \in \mathcal{R}_i$. All segments of S_i or T_i with an endpoint in R cross the boundary of R.*

As each vertex can only be endpoint of two segments in S_i and of two segments in T_i, there are only $\mathcal{O}(n)$ *start segments* in S_i and T_i , i.e., segments directly incident to a vertex. Hence, we only consider the bends of edges with both a middle segment in S_i and a middle segment in T_i where *middle segments* are segments which are not start segments. Refer to Fig. 10a for an illustration of such an edge. We refer to bends that are endpoints of a middle segment in S_i and of a start segment as *S_i-endpoints*. Analogously, we define *T_i-endpoints*.

▶ **Observation 10.** *Let $e \in E$ be an edge with two middle segments from S_i and T_i. The corresponding S_i- and T_i-endpoints are located in two disjoint regions of $\mathcal{R}_i$.*

Based on Observation 10, consider S_i- and T_i-endpoints in a region $R \in \mathcal{R}_i$ independently. Let $ep_{S_i}(R)$ ($ep_{T_i}(R)$) denote the set of S_i-endpoints (T_i-endpoints, resp.) in R. Further, $ep_{S_i}(R)$ can be subdivided into $ep^+_{S_i}(R)$, i.e. the set of S_i-endpoints that are the bottom endpoints of their corresponding S_i-segment, and $ep^-_{S_i}(R)$, i.e. the set of S_i-endpoints that are the corresponding top endpoints; see Fig. 10b. In other words, the S_i-segment incident to an endpoint in $ep^+_{S_i}(R)$ leaves R in positive y direction. Similarly, we subdivide $ep_{T_i}(R)$ into $ep^+_{T_i}(R)$ and $ep^-_{T_i}(R)$.

The segments in S_i and T_i form obstacles for possible connections of S_i- and T_i-endpoints to vertices. As a result, we will identify regions which have a visibility to many of the vertices connected to one of the sets of endpoints of region R, say $ep^+_{S_i}(R)$, to which we refer as *tunnels*. The *S_i-tunnel* $tun_{S_i}(R)$ of R is the region bounded by two lines parallel to the segments in S_i enclosing R. Further, $tun_{S_i}(R)$ is split by R into *S_i^+-tunnel* $tun^+_{S_i}(R)$ below R (see Fig. 10c) and the *S_i^--tunnel* $tun^-_{S_i}(R)$ above R. Similarly, we define T_i-tunnels for R.

Next, we define so-called *plausible* positions for all but $o(n)$ vertices connected to bends in $ep^+_{S_i}(R)$; the following analysis can be analogously adapted for bends in $ep^-_{S_i}(R)$. To realize those connections, bends have to be connected to some vertices by a start segment. Consider the set of slopes $A = \{0, 1/4, 1/2, 3/4, 1, 4/3, 2, 4, \infty\}$ and the two slopes $s_\ell \in A$ and $s_r \in A$ closest to the slope p/q of segments in S_i; see Figure 11a. Further, let α_ℓ denote the angle between slopes s_ℓ and p/q and α_r the angle between slopes s_r and p/q. Observe that $0 < \alpha_\ell, \alpha_r < \pi/4$. The choice of slopes in A is arbitrary and is simply used to discretize the slope p/q with a new slope whose nominator and denominator can be both expressed as a constant. For a bend b in $ep^+_{S_i}(R)$, we define a region of *S_i^+-plausible positions* by a wedge opposite to the attached S_i-segment delimited by two rays of slopes s_ℓ and s_r, resp.; see

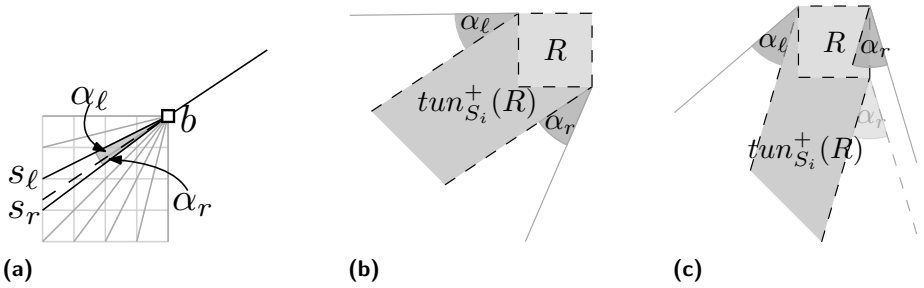

Figure 11 (a) Wedge of angle $\alpha_\ell + \alpha_r$ at bend $b \in ep^+_{S_i}(R)$ yielding S_i^+-plausible positions for b. (b)–(c) S_i^+-plausible region $plaus^+_{S_i}(R)$ of R, for different slopes of segments in S_i.

Fig. 11a. The union of the plausible positions of all bends in $ep^+_{S_i}(R)$ defines the *S_i^+-plausible region* $plaus^+_{S_i}(R)$ of R and consists of the union of R, $tun^+_{S_i}(R)$ and two attached wedges of angles α_ℓ and α_r, resp., on both sides of $tun^+_{S_i}(R)$. Observe these two wedges may be attached to two adjacent or two opposite corners of R depending on the slope of segments in S_i; see Figs. 11b and 11c. S_i^--, T_i^+- and T_i^--plausible regions are defined analogously.

▶ **Lemma 11.** *Let Γ be a RAC$_3$ drawing of K_n in $\mathcal{O}(n^2)$ area and let R be a region such that w.l.o.g. $|ep^+_{S_i}(R)| = \Omega(n^2)$. Vertices outside of $plaus^+_{S_i}(R) \cup tun^-_{S_i}(R)$ are directly connected to only $\mathcal{O}(n)$ bends in $ep^+_{S_i}(R)$ in total.*

Proof. The segments in S_i can only be crossed by segments of T_i. There are at most two start segments for each vertex that belong to T_i, hence, only two start segments of each vertex can cross segments of S_i. Those can be neglected as they are only $\mathcal{O}(n)$ segments and, in the following, we only consider start segments with different slopes. Consider an S_i-endpoint b and assume that b is connected to vertex v outside of $plaus^+_{S_i}(R) \cup tun^-_{S_i}(R)$. Assume w.l.o.g. that v is to the left of $plaus^+_{S_i}(R) \cup tun^-_{S_i}(R)$. The segment connecting b and v has a slope diverging by more than α_ℓ from slope p/q. Hence, b may be attached to a vertex v to the left of $plaus^+_{S_i}(R)$ only if a ray of slope s_ℓ with right endpoint b does not cross any segment in S_i with endpoint in $ep^+_{S_i}(R)$. This is true because the segment between b and v will intersect at least the segments that are also intersected by the ray of slope s_ℓ.

Consider the set of S_i-endpoints B for which such a crossing-free ray of slope s_ℓ exists; see Fig. 12a. Note that all rays are parallel and do not overlap. Since all possible slopes $s_\ell \in A$ can be expressed as a quotient p_ℓ/q_ℓ for $p_\ell, q_\ell \in \mathcal{O}(1)$ and since all rays hit one integer point, the minimum distance between two such parallel rays is $\Omega(1)$. Since R has size $\mathcal{O}(n) \times \mathcal{O}(n)$, it follows that there are only $\mathcal{O}(n)$ parallel rays of slope s_ℓ and hence $|B| = \mathcal{O}(n)$. ◀

In the following, we consider a region R and its set of *neighbored regions* $\mathcal{N}(R)$. A neighbored region $R' \in \mathcal{N}(R)$ is a region obtained by shifting R $c_1 q + c_2 p$ units along the x-axis and $c_1 p - c_2 q$ units along the y-axis for integers c_1, c_2; see Fig. 12b. Note that $\mathcal{N}(R)$ contains projections of $R \in \mathcal{R}_i$ that are not necessarily part of $\mathcal{R}_i$. Region R' contains all T_i-endpoints that are reached from S_i-endpoints in R by a segment in S_i with length $|c_1| \cdot \sqrt{p^2+q^2}$ followed by a segment in T_i of length $|c_2| \cdot \sqrt{p^2+q^2}$. Assume w.l.o.g. that $c_1, c_2 > 0$. Then, the edges with S- and T-endpoints in R and R', resp., will have a bend in $ep^+_{S_i}(R)$ and $ep^+_{T_i}(R')$. The symmetric cases where $c_1 < 0$ or $c_2 < 0$ are analogous. We say that a vertex v is an *R-vertex* if it is directly connected to $\Omega(n)$ bends in $ep^+_{S_i}(R)$ but to only $o(n)$ bends in $ep^+_{T_i}(R')$. Conversely, we say that v is an *R'-vertex* if it is directly connected to $\Omega(n)$ bends in $ep^+_{T_i}(R')$ but to only $o(n)$ bends in $ep^+_{S_i}(R)$. In the following, we show that except for $\mathcal{O}(n)$ edges, the edges with S- and T-endpoints in neighbored regions

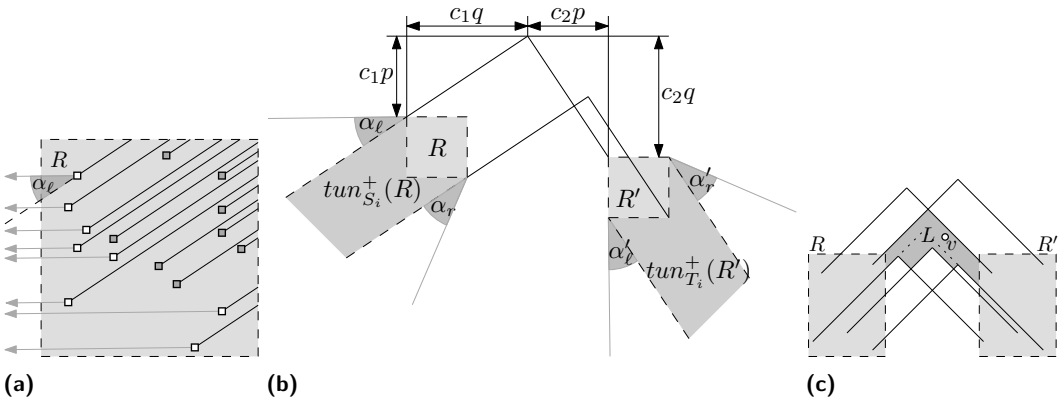

Figure 12 (a) Rays of slopes s_ℓ (arrows) attached to bends visible from outside $plaus^+_{S_i}(R) \cup tun^-_{S_i}(R)$. (b) Illustration of a region R and one of its neighbored regions R'. (c) Illustration of an L-tunnel L between region R and $R' \in \mathcal{N}(R)$ with a vertex v.

induce a bipartite subgraph between R- and R'-vertices. We refer to those exceptional edges which are either connecting two R- or R'-vertices or have an endpoint which is neither R- nor R'-vertex as *complete edges*. Intuitively speaking, a complete edge connects the set of R- and R'-vertices which are otherwise behaving like the partitions of a bipartite graph. In particular, every complete edge

(i) is either incident to a vertex which is neither R- nor R'-vertex, or
(ii) has a start segment that connects an R-vertex with a bend in $ep^+_{T_i}(R')$, or,
(iii) has a start segment that connects an R'-vertex with a bend in $ep^+_{S_i}(R)$.

We refer to the special endpoint as a *complete* endpoint. We first show that vertices in the intersection of $tun^-_{S_i}(R)$ and $tun^-_{T_i}(R')$ can be complete endpoint for only $\mathcal{O}(n)$ edges. Later, we will consider the case where vertices are not located in the intersection of $tun^-_{S_i}(R)$ and $tun^-_{T_i}(R')$. Consider a vertex v located in the intersection $tun^-_{S_i}(R) \cap tun^-_{T_i}(R')$ in a so-called *L-tunnel* between R and R'. An L-tunnel is a region bounded by edges with S- and T-endpoints in R and R', resp., that is open to both R and R' such that v can see into regions R and R'; see Fig. 12c. More precisely, an L-tunnel L is an open subregion of $tun^-_{S_i}(R) \cap tun^-_{T_i}(R')$ bounded from below by an alternating sequence of S_i and T_i segments between R and R' and from above by two segments, one from S_i and one from T_i, while it is bounded to the left by the boundary of R and to the right by the boundary of R'.

▶ **Lemma 12.** *Let Γ be a RAC$_3$ drawing of K_n in $\mathcal{O}(n^2)$ area, let R be a region such that w.l.o.g. $|ep^+_{S_i}(R)| = \Omega(n^2)$ and let $R' \in \mathcal{N}(R)$. There are $\mathcal{O}(n)$ complete edges with both a bend in $ep^+_{S_i}(R)$ and in $ep^+_{T_i}(R')$ whose complete endpoints are an in L-tunnels in $tun^-_{S_i}(R) \cap tun^-_{T_i}(R')$.*

Proof. Let v be a complete endpoint in $tun^-_{S_i}(R) \cap tun^-_{T_i}(R')$, hence, it is connected to bends in $ep^+_{S_i}(R)$ and to bends in $ep^+_{T_i}(R')$. Further, assume that v is complete endpoint for at least two edges; the complete endpoints that we disregard only contribute $\mathcal{O}(n)$ edges. Assume w.l.o.g. that the slope of segments in S_i is less than 1. Then, the slope of segments in T_i is less than -1 and v is located above R'. Let $B(v)$ denote the set of bends that v is connected to in $ep^+_{T_i}(R')$. We further divide $B(v)$ into $B^-(v)$ and $B^+(v)$, i.e., the set of bends b such that v is located in the halfplane above and below b's segment in T_i, resp. We first show, that each $b \in B^\pm(v)$ shares its y-coordinate with no other bend $b' \in B^\pm(v)$. Then, we show that for two vertices v and v' in $tun^-_{S_i}(R) \cap tun^-_{T_i}(R')$, the y-coordinates of bends in $B^\pm(v)$ and $B^\pm(v')$ differ. As a result, there are only $\mathcal{O}(n)$ bends in R', which implies that there are only $\mathcal{O}(n)$ complete edges.

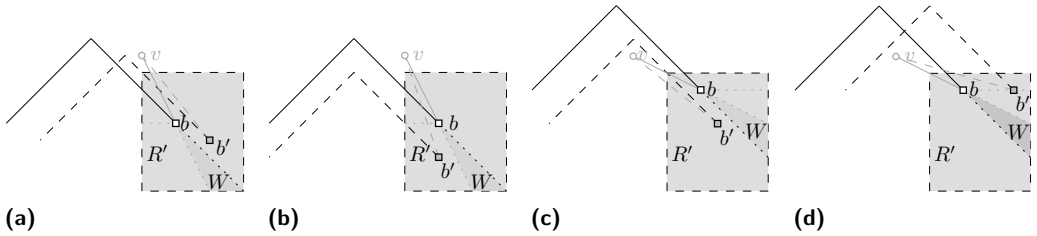

Figure 13 A bend b incident to a vertex v restricts the position of other bends b' to a wedge W.

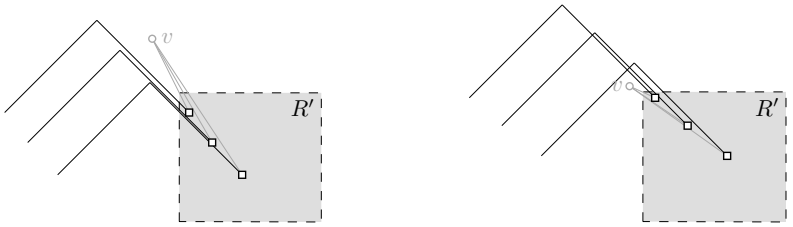

Figure 14 (a) Edges below a vertex v incident to v do not intersect while (b) edges above a vertex v incident to v pairwise intersect.

Consider a vertex v and a bend $b \in B(v)$. First, assume that $b \in B^-(v)$. Note that since v is located above R' in the intersection $tun^-_{S_i}(R) \cap tun^-_{T_i}(R')$, the segment between b and v has slope less than -1. Then v can only be incident to another bend $b' \in B^-(v)$ whose T_i-segment is below v only if b' is located in the wedge W obtained by the elongation of the T_i-segment of b and the segment between b and v. Otherwise the T_i-segment incident to b' would intersect the segment between b and v (see Fig. 13a) or the segment between b' and v would intersect the T_i-segment incident to b (see Fig. 13b). Since the angle between the two segments spanning the wedge W from above is less than π, W contains no other bend with the same y-coordinate as b. Moreover, we observe that the T_i-segments incident to such bends and consecutive S_i-segments do not cross each other (see Fig. 14a) since all S_i-(T_i-, resp.)segments between R and R' have the same length. Second, consider the case where $b \in B^+(v)$. Here, the argumentation is analogous to the previous case (see Figs. 13c and 13d). Note that in this case, the edges using bends in $B^+(v)$ pairwise intersect (see Fig. 14b). Still segments incident to v have negative slopes.

It remains to consider the dependencies of the neighborhoods of two vertices v and v' located in $tun^-_{S_i}(R) \cap tun^-_{T_i}(R')$. First, consider the positions of bends in $B^-(v)$ and of bends in $B^-(v')$. There are three possibilities for the relative positioning of v and v':

1. v and v' appear in different L-tunnels such that w.l.o.g. the L-tunnel of v' appears below the bottommost bend $b_{bot}(v) \in B^-(v)$. Then v' appears in the halfplane below the segment in T_i attached to $b_{bot}(v)$. Even more, the topmost bend $b_{top}(v') \in B^-(v')$ must be located below v'; see Fig 15a. Hence, the y-coordinates of $B^-(v)$ and $B^-(v')$ are different.
2. v and v' appear in the same L-tunnel. W.l.o.g. the topmost bend $b_{top}(v') \in B^-(v')$ will be located in a wedge W below $b_{bot}(v) \in B^-(v)$ delimited by the elongation of the T_i-segment through $b_{bot}(v)$ and a horizontal through $b_{bot}(v)$; see Fig. 15b. The horizontal segment delimits W as by the choice of the size of regions, v' will be located above R', hence it also does not belong to W. Therefore, y-coordinates of $B^-(v)$ and $B^-(v')$ differ.

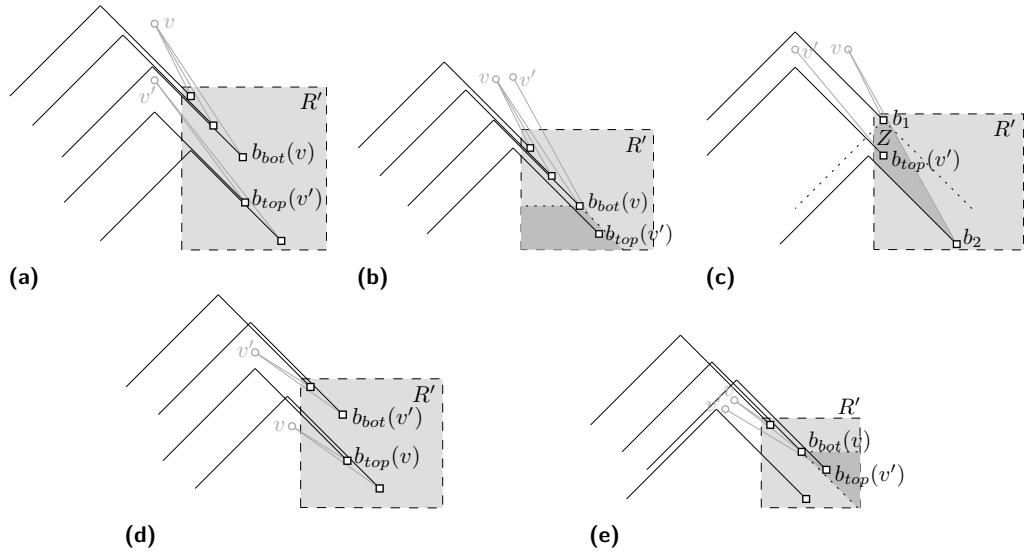

Figure 15 (a)–(c) Bends in $B^-(v)$ and bends in $B^-(v')$ have different y-coordinates. (d)–(e) Bends in $B^+(v)$ and bends in $B^+(v')$ have different y-coordinates.

3. v' is located in between the T_i-segments incident to $b_1, b_2 \in B^-(v)$. The bends in $B^-(v')$ can only be located in a region Z bounded by two lines of the slopes of S_i and T_i passing through b_1, the T_i-segment incident to b_2, the segment between v and b_2 and the boundary of region R'. All points in this region have smaller y-coordinates than b_1 and larger y-coordinates than b_2; see Fig. 15c. Note that the line parallel to segments of S_i passing through b_1 is part of the boundary as otherwise the segments incident to b_1 and a bend in $B^-(v')$, resp., would intersect preventing v' from having segments to bends in R.

Second, consider how the positions of bends in $B^+(v)$ and bends in $B^+(v')$ depend on each other. Here, there are only two possibilities for the relative positioning of v and v' which are analogous to the Cases 1 and 2 above, see Figs. 15d and 15e.

Note that a bend in $\bigcup_v B^-(v)$ and in $\bigcup_v B^+(v)$ may share a common y-coordinate. By the previous analysis, this is the only possibility for two bends in $\bigcup_v B(v)$ to share a y-coordinate. It follows that $|\bigcup_v B^-(v)| = \mathcal{O}(n)$ and $|\bigcup_v B^+(v)| = \mathcal{O}(n)$ and hence only a linear number of complete edges can be realized as claimed. ◀

Now, we summarize the partial results from Lemmas 11 and 12 to conclude that most vertices are R- or R'-vertices with only $\mathcal{O}(n)$ incident complete edges.

▶ **Lemma 13.** *Let Γ be a RAC$_3$ drawing of K_n in $\mathcal{O}(n^2)$ area. Further let R be a region such that w.l.o.g. $|ep^+_{S_i}(R)| = \Omega(n^2)$ and let $R' \in \mathcal{N}(R)$. Then there exist only $\mathcal{O}(n)$ complete edges that have a bend in $ep^+_{S_i}(R)$ and in $ep^+_{T_i}(R')$.*

Proof. Assume $tun^-_{S_i}(R)$ is delimited by the extension of two segments of S_i between R and R'. Otherwise, R can be restricted to a smaller region that only includes S_i-endpoints that are connected to T_i-endpoints located in R'. Assume that there are $\omega(n)$ complete edges with S- and T-endpoints in R and R', resp. By Lemma 12, there exist only $\mathcal{O}(n)$ complete edges with S- and T-endpoints in R and R', resp., whose complete endpoints are located in $tun^-_{S_i}(R) \cap tun^-_{T_i}(R')$. Since $tun^-_{S_i}(R)$ is bounded by two segments of S_i between R and R', this covers all complete endpoints in $tun^-_{S_i}(R) \cap tun^-_{T_i}(R')$ and other complete endpoints located in

$tun^-_{S_i}(R) \cup tun^-_{T_i}(R')$ lie outside of $plaus^+_{S_i}(R) \cup tun^-_{S_i}(R)$ or outside of $plaus^+_{T_i}(R') \cup tun^-_{T_i}(R')$. By Lemma 11, only $\mathcal{O}(1)$ vertices outside of $plaus^+_{S_i}(R) \cup tun^-_{S_i}(R)$ can each be connected to $\Omega(n)$ bends of $ep^+_{S_i}(R)$, also only $\mathcal{O}(1)$ vertices outside of $plaus^+_{T_i}(R') \cup tun^-_{T_i}(R')$ can each be connected to $\Omega(n)$ bends of $ep^+_{T_i}(R')$. Thus, there must be complete endpoints in $plaus^+_{S_i}(R) \cap plaus^+_{T_i}(R')$ contradicting $plaus^+_{S_i}(R) \cap plaus^+_{T_i}(R') = \emptyset$. ◀

Lemma 13 shows, that most edges with S- and T-endpoints in R and R', resp., define a bipartite subgraph. As a result, edges between R and $\mathcal{N}(R)$ define a p-partite subgraph for some constant $p > 1$. However, since the drawn graph is complete, all R-vertices have to define a clique. This will lead to a contradiction in the proof of the main theorem of this section.

▶ **Theorem 14.** *There is no RAC_3 drawing of K_n in $\mathcal{O}(n^2)$ area for sufficiently large n.*

Proof. Assume there is a RAC_3 drawing Γ of K_n in $\mathcal{O}(n^2)$ area. We show that there is a complete subgraph G' with $\Omega(n)$ vertices drawn in Γ with only $o(n^2)$ edges from E^{ST}_i for all pairs of perpendicular edge segments $S_i \in \mathcal{S}$ and $T_i \in \mathcal{T}$. This contradicts the property from Lemma 6 for the subdrawing of G'. Let c_{ST} denote the multiplicative constant from Lemma 6, i.e. $|E^{ST}_i| \geq c_{ST} n^2$.

We compute $G' = (V', E')$ iteratively. We initialize G' by G. We consider all pairs of sets of segments $S_i \in \mathcal{S}$ and $T_i \in \mathcal{T}$ with perpendicular slopes such that $|E^{ST}_i| \geq c_{ST} n^2$. There can be only a constant number of pairs of segment sets in $\mathcal{S}$ and $\mathcal{T}$ of size $\Omega(n^2)$. For each such pair, let $\mathcal{R}_i$ be a checkerboard partitioning of the drawing area into square-shaped disjoint regions of side length $\max\{p_i, q_i\}/2$ defined by slope p_i/q_i of S_i for coprime integers p_i and q_i. We consider all regions $R \in \mathcal{R}_i$. Due to the size of regions, there is only a constant number of regions in $\mathcal{R}_i$. Moreover, the number of neighbored regions $R' \in \mathcal{N}(R)$ is constant. Hence, there is a constant number n_{comb} of combinations of index i, region R and neighbored region R'.

We iteratively perform the following procedure while there are at least $c_{ST}|V'|^2$ edges with a bend in $ep^+_{S_i}(R)$ and a bend in $ep^{\pm}_{T_i}(R')$ for one of n_{comb} of combinations of index i, region R and neighbored region R' where $ep^{\pm}_{T_i}(R')$ is either $ep^+_{T_i}(R')$ or $ep^-_{T_i}(R')$ depending on the choice of R'. Let V_R denote the set of R- and $V_{R'}$ denote the set of R'-vertices. Assume w.l.o.g. that $|V_R| \geq |V_{R'}|$. By Lemma 13, the vertices that are neither R- nor R'-vertices are connected to $\mathcal{O}(n)$ bends in $ep^+_{S_i}(R)$, $ep^+_{T_i}(R')$ or $ep^-_{T_i}(R')$ in total. More precisely, there are $c_{comp}|V'|$ such bends for an appropriately chosen constant c_{comp}. Recall that vertices that are not incident to $\Omega(n)$ bends, say at least $c_R|V^*|$ for an appropriately chosen constant c_R, in $ep^+_{S_i}(R)$ and $ep^+_{T_i}(R')$ are either R- or R'-vertex for the resulting graph $G^* = (V^*, V^* \times V^*)$. By the prior observation, $|V_R| = \Omega(n)$, more precisely, $|V_R| \geq (|V'| - c_{comp}|V'|/c_R|V^*|)/2$. We then continue to consider the complete subgraph induced by V_R. Note that since n_{comb} is constant, by Lemma 13, this subgraph and the subgraphs in the future iterations contain only $\mathcal{O}(n)$ edges with both a segment in S_i and a segment in T_i and bends in $ep^+_{S_i}(R)$ and $ep^+_{T_i}(R')$ or $ep^-_{T_i}(R')$ for all $R' \in \mathcal{N}(R)$ for sufficiently large n. Thus, we set $G' \leftarrow (V_R, V_R \times V_R)$ and continue with the next iteration.

After performing all at most n_{comb} iterations, there are less than $c_{ST}|V'|^2$ edges with both a bend in $ep^+_{S_i}(R)$ and a bend in $ep^+_{T_i}(R')$ and $ep^-_{T_i}(R')$ for all combinations of index i, region $R \in \mathcal{R}_i$ and neighbored region $R' \in \mathcal{N}(R)$. Hence, the resulting subgraph G' is drawn with $|E^{ST}_i| < c_{ST}|V'|^2$ for each pair of sets of segments $S_i \in \mathcal{S}$ and $T_i \in \mathcal{T}$ with perpendicular slopes which contradicts Lemma 6. ◀

Our proofs explicitly use the assumption of quadratic area (Lemmas 8 to 12) and three bends per edge (Lemmas 11 to 13). Even for $\omega(n^2)$ area, our proof does not apply.

4 Open Questions

We raise the following open questions:

(i) How many bends are needed for achieving quadratic area RAC drawings? We showed that three are insufficient and that eight are enough.

(ii) Is cubic area optimal for RAC_3 drawings? Our lower bound proof might be extendable.

(iii) Is quadratic area achievable in simple RAC drawings? In *simple drawings*, every pair of edges shares at most one point (crossing or endpoint); a property our algorithms do not guarantee.

References

1 M. Ajtai, V. Chvátal, M. M. Newborn, and E. Szemerédi. Crossing-free subgraphs. In *Theory and practice of combinatorics*, volume 60 of *North-Holland Math. Stud.*, pages 9–12. North-Holland, Amsterdam, 1982.

2 Patrizio Angelini, Michael A. Bekos, Henry Förster, and Michael Kaufmann. On rac drawings of graphs with one bend per edge. *Theoretical Computer Science*, 2020. doi:10.1016/j.tcs.2020.04.018.

3 Patrizio Angelini, Luca Cittadini, Walter Didimo, Fabrizio Frati, Giuseppe Di Battista, Michael Kaufmann, and Antonios Symvonis. On the perspectives opened by right angle crossing drawings. *J. Graph Algorithms Appl.*, 15(1):53–78, 2011. doi:10.7155/jgaa.00217.

4 Patrizio Angelini, Giuseppe Di Battista, Walter Didimo, Fabrizio Frati, Seok-Hee Hong, Michael Kaufmann, Giuseppe Liotta, and Anna Lubiw. Large angle crossing drawings of planar graphs in subquadratic area. In Alberto Márquez, Pedro Ramos, and Jorge Urrutia, editors, *Computational Geometry - XIV Spanish Meeting on Computational Geometry, EGC 2011, Dedicated to Ferran Hurtado on the Occasion of His 60th Birthday*, volume 7579 of *Lecture Notes in Computer Science*, pages 200–209. Springer, 2011. doi:10.1007/978-3-642-34191-5_19.

5 Evmorfia N. Argyriou, Michael A. Bekos, and Antonios Symvonis. The straight-line RAC drawing problem is np-hard. *J. Graph Algorithms Appl.*, 16(2):569–597, 2012. doi:10.7155/jgaa.00274.

6 Karin Arikushi, Radoslav Fulek, Balázs Keszegh, Filip Moric, and Csaba D. Tóth. Graphs that admit right angle crossing drawings. *Comput. Geom.*, 45(4):169–177, 2012. doi:10.1016/j.comgeo.2011.11.008.

7 Christian Bachmaier, Franz J. Brandenburg, Kathrin Hanauer, Daniel Neuwirth, and Josef Reislhuber. NIC-planar graphs. *Discrete Applied Mathematics*, 232:23–40, 2017. doi:10.1016/j.dam.2017.08.015.

8 Michael A. Bekos, Walter Didimo, Giuseppe Liotta, Saeed Mehrabi, and Fabrizio Montecchiani. On RAC drawings of 1-planar graphs. *Theor. Comput. Sci.*, 689:48–57, 2017. doi:10.1016/j.tcs.2017.05.039.

9 Franz J. Brandenburg, Walter Didimo, William S. Evans, Philipp Kindermann, Giuseppe Liotta, and Fabrizio Montecchiani. Recognizing and drawing IC-planar graphs. *Theor. Comput. Sci.*, 636:1–16, 2016. doi:10.1016/j.tcs.2016.04.026.

10 Steven Chaplick, Fabian Lipp, Alexander Wolff, and Johannes Zink. Compact drawings of 1-planar graphs with right-angle crossings and few bends. *Comput. Geom.*, 84:50–68, 2019. doi:10.1016/j.comgeo.2019.07.006.

11 Emilio Di Giacomo, Walter Didimo, Peter Eades, and Giuseppe Liotta. 2-layer right angle crossing drawings. *Algorithmica*, 68(4):954–997, 2014. doi:10.1007/s00453-012-9706-7.

12 Emilio Di Giacomo, Walter Didimo, Giuseppe Liotta, and Henk Meijer. Area, curve complexity, and crossing resolution of non-planar graph drawings. *Theory Comput. Syst.*, 49(3):565–575, 2011. doi:10.1007/s00224-010-9275-6.

13 Emilio Di Giacomo, Walter Didimo, Giuseppe Liotta, and Fabrizio Montecchiani. Area requirement of graph drawings with few crossings per edge. *Comput. Geom.*, 46(8):909–916, 2013. doi:10.1016/j.comgeo.2013.03.001.

14 Emilio Di Giacomo, Walter Didimo, Giuseppe Liotta, and Fabrizio Montecchiani. Area-thickness trade-offs for straight-line drawings of planar graphs. *Comput. J.*, 60(1):135–142, 2017. doi:10.1093/comjnl/bxw075.

15 Walter Didimo, Peter Eades, and Giuseppe Liotta. Drawing graphs with right angle crossings. *Theor. Comput. Sci.*, 412(39):5156–5166, 2011. doi:10.1016/j.tcs.2011.05.025.

16 Vida Dujmović, Joachim Gudmundsson, Pat Morin, and Thomas Wolle. Notes on large angle crossing graphs. *Chicago J. Theor. Comput. Sci.*, 2011, 2011. URL: http://cjtcs.cs.uchicago.edu/articles/CATS2010/4/contents.html.

17 Christian A. Duncan and Michael T. Goodrich. Planar orthogonal and polyline drawing algorithms. In Roberto Tamassia, editor, *Handbook on Graph Drawing and Visualization*, pages 223–246. Chapman and Hall/CRC, 2013.

18 Peter Eades and Giuseppe Liotta. Right angle crossing graphs and 1-planarity. *Discrete Applied Mathematics*, 161(7-8):961–969, 2013. doi:10.1016/j.dam.2012.11.019.

19 Seok-Hee Hong and Hiroshi Nagamochi. Testing full outer-2-planarity in linear time. In Ernst W. Mayr, editor, *Graph-Theoretic Concepts in Computer Science - 41st International Workshop, WG 2015*, volume 9224 of *Lecture Notes in Computer Science*, pages 406–421. Springer, 2015. doi:10.1007/978-3-662-53174-7_29.

20 Weidong Huang. Using eye tracking to investigate graph layout effects. In Seok-Hee Hong and Kwan-Liu Ma, editors, *APVIS 2007, 6th International Asia-Pacific Symposium on Visualization 2007*, pages 97–100. IEEE Computer Society, 2007. doi:10.1109/APVIS.2007.329282.

21 Weidong Huang, Peter Eades, and Seok-Hee Hong. Larger crossing angles make graphs easier to read. *J. Vis. Lang. Comput.*, 25(4):452–465, 2014. doi:10.1016/j.jvlc.2014.03.001.

22 Frank Thomson Leighton. *Complexity Issues in VLSI*. Foundations of Computing Series. MIT Press, Cambridge, MA, 1983.

23 János Pach and Géza Tóth. Graphs drawn with few crossings per edge. *Combinatorica*, 17(3):427–439, 1997. doi:10.1007/BF01215922.

24 Helen C. Purchase. Effective information visualisation: a study of graph drawing aesthetics and algorithms. *Interacting with Computers*, 13(2):147–162, 2000. doi:10.1016/S0953-5438(00)00032-1.

25 Helen C. Purchase, David A. Carrington, and Jo-Anne Allder. Empirical evaluation of aesthetics-based graph layout. *Empirical Software Engineering*, 7(3):233–255, 2002.

26 Zahed Rahmati and Fatemeh Emami. RAC drawings in subcubic area. *Information Processing Letters*, 159-160:105945, 2020. doi:10.1016/j.ipl.2020.105945.